Transverse mode control by etch-depth tuning in 1120-nm GaInAs/GaAs photonic crystal vertical-cavity surface-emitting lasers

Jong-Hwa Baek, Dae-Sung Song, In-Kag Hwang, Kum-Hee Lee, and Y. H. Lee

Department of Physics, Korea Advanced Institute of Science and Technology, Daejeon 305-701, Korea
baekjhing@empal.com

Young-gu Ju

Electronics and Telecommunications Research Institute, Daejeon 305-350, Korea

Takashi Kondo, Tomoyuki Miyamoto, and Fumio Koyama

Precision and Intelligence Laboratory, Tokyo Institute of Technology, Yokohama 226-8503, Japan

Abstract: Robust and tolerant single-transverse-mode photonic crystal GaInAs vertical-cavity surface-emitting lasers are fabricated and investigated. Triangular lattice patterns of rectangular air holes of various etch-depths are introduced in the top mirror. The stable single-transverse-mode operation is observed with a large margin of allowance in the etch depth ($t = 2.5 \pm 0.6$ μm). This stable mode selection mechanism is explained by the mode competition between the two lowest photonic crystal guided modes that are influenced by both the index guiding effect and the etch-depth dependent modal losses.

OCIS codes: (250.7260) Vertical cavity surface emitting lasers; (230.0250) Optoelectronics.

References and links

1. S. Sato, N. Nishiyama, T. Miyamoto, T. Takahashi, N. Jikutani, M. Arai, A. Matsutani, F. Koyama, and K. Iga, "Continuous wave operation of 1.26 μm GaInNAs/GaAs vertical-cavity surface-emitting lasers grown by metalorganic chemical vapour deposition," Electron. Lett. **36,** 2018-2019 (2000).
2. T. Kageyama, T. Miyamoto, S. Makino, Y. Ikenaga, N. Nishiyama, A. Matsutani, F. Koyama, and K. Iga, "Room temperature continuous-wave operation of GaInNAs/GaAs VCSELs grown by chemical beam epitaxy with output power exceeding 1 mW," Electron. Lett. **37,** 225-226 (2001).
3. T. Anan, M. Yamada, K. Nishi, K. Kurihara, K. Tokutome, A. Kamei, and S. Sugou, "Continuous-wave operation of 1.30 μm GaAsSb/GaAs VCSELs," Electron. Lett. **37,** 566-567 (2001).
4. Z. Zou, D. L. Huffaker, S. Csutak, and D. G. Deppe, "Ground state lasing from a quantum-dot oxide-confined vertical-cavity surface-emitting laser," Appl. Phys. Lett. **75,** 22-24 (1999).
5. J. A. Lott, N. N. Ledentsov, V. M. Ustinov, N. A. Maleev, A. E. Zhukov, A. R. Kovsh, M. V. Maximov, B. V. Volovik, ZH. I. Alferov, and D. Bimberg, "InAs-InGaAs quantum dot VCSELs on GaAs substrates emitting at 1.3 μm," Electron. Lett. **36,** 1384-1385 (2000).
6. T. Kondo, M. Arai, M. Azuchi, T. Uchida, A. Matsutani, T. Miyamoto, and F. Koyama, "Low threshold current density operation of 1.16 μm highly strained GaInAs/GaAs vertical-cavity surface-emitting lasers on (100) GaAs substrate," Jpn. J. Appl. Phys. **41,** L562-L564 (2002).
7. F. Koyama, D. Schlenker, T. Miyamoto, Z. Chen, A. Matsutani, T. Sakaguchi, and K. Iga, "Data transmission over single-mode fiber by using 1.2-μm uncooled GaInAs-GaAs laser for Gb/s local area network ," IEEE Photon. Technol. Lett. **12,** 125-127 (2000).
8. D. S. Song, S. H. Kim, H. G. Park, C. K. Kim, and Y. H. Lee, "Single-fundamental-mode photonic-crystal vertical-cavity surface-emitting laser," Appl. Phys. Lett. **80,** 3901-3903 (2002).
9. D. S. Song, Y. J. Lee, H. W. Choi, and Y. H. Lee, "Polarization-controlled, single-transverse-mode, photonic-crystal, vertical-cavity surface-emitting lasers," Appl. Phys. Lett. **82,** 3182-3184 (2003).
10. N. Yokouchi, A. J. Danner, and K. D. Choquette, "Vertical-cavity surface-emitting laser operating with photonic crystal seven-point defect structure," Appl. Phys. Lett. **82,** 3608-3610 (2003).

#3764 - $15.00 US Received 3 February 2004; revised 25 February 2004; accepted 26 February 2004

11. J. W. Matthews, and A. E. Blakeslee, "Defects in epitaxial multilayers : l. Misfit dislocations," J. Cryst. Growth. **27,** 118-125 (1974).
12. D. Schlenker, T. Miyamoto, Z. Chen, M. Kawaguchi, T. Kondo, E. Gouards, F. Koyama, and K. Iga, "Critical layer thickness of 1.2-μm highly strained GaInAs/GaAs qusntum wells," J. Cryst. Growth. **221,** 503-508 (2000).
13. T. A. Birks, J. C. Knight, and P. St. J. Russell, "Endlessly single-mode photonic crystal fiber," Opt. Lett. **22,** 961-963 (1997).

1. Introduction

Mode-controlled long-wavelength vertical-cavity surface-emitting lasers (VCSELs) are dearly sought after for high-speed local-area networks and metropolitan-area networks applications. These VCSELs have been known as the strong candidate of the low cost source that can extend the reach of current 850-nm based data communication links to the longer distance necessary for the metro/access market. There have been strong on-going efforts for long-wavelength VCSELs based on InGaAsP/InP material systems. Together with these approaches, various GaAs-based systems such as GaInNAs/GaAs quantum well (QW) [1,2], GaAsSb/GaAs QW [3], and GaInAs/GaAs quantum dots [4,5] have also been employed for long-wavelength (1300 – 1500 nm) VCSELs. Moreover, experimentally, highly-strained GaInAs/GaAs QW lasers [6] have reached the wavelength >1,200 nm. In fact, 1200-nm VCSELs have the possibility of transmitting data at 10 Gb/s over 10 km [7]. In other words, highly-strained GaInAs/GaAs VCSELs armed with the single-transverse mode should be a good candidate for medium- to long-reach applications.

Previously, the dependable single transverse mode operation has been demonstrated from 850-nm photonic-crystal vertical-cavity surface-emitting lasers (PC-VCSELs) [8]. These PC-VCSELs are similar to standard VCSELs except that they have photonic crystal patterns defined by air-holes drilled about half-way into the top mirror region [8-10]. Although the selection of the single transverse mode was obtained with relative ease, the detailed mode selection mechanisms are not yet understood.

In this letter, the origin of transverse mode selection mechanisms of PC-VCSELs is studied. As we vary the air-hole depths, the stable single transverse mode operation is observed over a wide range of etch depth. The experimental data and the influence of the effective wave-guiding and the etched top DBR are discussed to understand the physics of the transverse mode selection.

2. Design and fabrication

The highly-strained GaInAs/GaAs VCSEL wafer was grown by MOCVD. The bottom n-type distributed Bragg reflector (DBR) consisted of 35.5 pairs of GaAs(80.5nm)/$Al_{0.8}Ga_{0.2}As$(91.4nm) on GaAs substrate. The top p-type DBR consisted of 22 pairs of GaAs/$Al_{0.8}Ga_{0.2}As$. A 30-nm-thick $Al_{0.98}Ga_{0.02}As$ layer for oxidation was introduced in the upper mirror. The active region consisted of 8-nm-thick $Ga_{0.68}In_{0.32}As$ 3QWs that were compressively strained and 25-nm-thick GaAs barriers. GaAs spacer layers surrounded this region to form a λ-cavity. The thickness of QWs is larger than the critical thickness of QWs [11]. However, a high-quality material is achievable by suppression of the transition to the three-dimensional growth [12]. The fabrication process of the PC-VCSEL is similar to that of the conventional VCSEL. The 60-μm-wide mesa was formed by chemical assisted ion beam etching (CAIBE) and the 30-nm-thick $Al_{0.98}Ga_{0.02}As$ layer was oxidized, air-holes were etched by CAIBE, and finally both electrodes were coated. Fig. 1 gives the top view of a fabricated PC-VCSEL. The lattice constant of the triangular photonic crystal pattern was fixed at 5 μm. Several sizes of rectangular air-holes (3.5×2 μm^2, 3.5×2.2 μm^2, 3.5×2.4 μm^2) and samples of various etch depths (5, 8, 15, 18, >22 pairs of GaAs/$Al_{0.8}Ga_{0.2}As$ layers) were prepared. These values were chosen based on a previous work for single transverse mode operation [9]. VCSELs without air-holes were also prepared as a reference sample. For current limiting, an oxide aperture of diameter 16 μm was formed by wet oxidation techniques. The oxide aperture had nearly the same diameter as the inner circle of the top electrode that was large

#3764 - $15.00 US Received 3 February 2004; revised 25 February 2004; accepted 26 February 2004

enough to decouple the unwanted index guiding contribution from the current limiting oxide aperture.

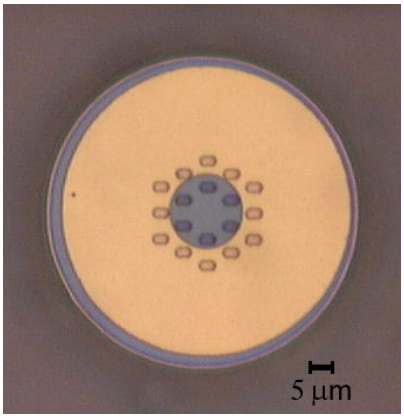

Fig. 1. Top view of the fabricated PC-VCSEL with rectangular air-holes.

3. Experimental results

In general, characteristic behaviors of the PC-VCSELs were found not to depend sensitively on the size of photonic crystal air-holes. Consequently, we focused our attention to the effect of the etch depth by choosing a photonic crystal pattern with an air-hole size of 3.5×2.4 μm^2 and a lattice constant of 5 μm for subsequent analyses.

Output spectra and near-field CCD mode patterns at-threshold and above-threshold were measured and shown in Fig. 2 and Fig. 3. The reference VCSEL without air-holes operated in multi-modes over the entire current range, as is commonly expected from a typical 16-μm VCSEL, as shown in Fig. 2(a).

Shallow-etch samples (5-, 8-pairs of GaAs/$Al_{0.8}Ga_{0.2}$As etched layers) operated in the single transverse mode only near the threshold. However, with slightly higher current, many higher-order transverse modes showed up as shown in Figs. 2(b), (c). Interestingly, the spot diameter (10μm) under the multi-mode operation was much larger than that (3.8μm) under the single mode operation. In our experiment, the spot diameter is defined at 1/e points of the transverse mode profile that is obtained from the Fourier transformation of the measured far field profile. Under the multi-mode operation regime, the shallow-etch sample showed the mode size comparable to that of the reference VCSEL as shown in Fig. 3, implying the insufficient index guiding introduced by the shallow-etched air-holes.

On the other hand, all the mid-etch samples (12-, 15-, 18-pair GaAs/$Al_{0.8}Ga_{0.2}$As etched layers) operated in the single and fundamental transverse mode over the entire operating current range, as shown in Figs. 2(d) - (f). Numerically, these etch depths lie between 1.9 μm and 3.1 μm, which promises a generous fabrication tolerance on the etch depth. The measured mode size of the fundamental mode decreased slightly with the etch depth. The actual mode diameters were 3.78, 3.74, and 3.63 μm for 12-, 15-, and 18-pair mid-etch samples, respectively. The mode diameters of 12-pair mid-etch sample were measured at various currents, also, which were 3.78, 3.42, and 3.07 μm at 4, 8, and 12mA, respectively. In general, the state of polarization was determined by the orientation of the rectangular air-holes, as shown in Fig. 4, consistent with that in Ref. [9]. It is encouraging to report that the most (95%) of the PC-VCSELs with rectangular air-holes operated in the single polarization, single-transverse mode with the polarization suppression ratio of > 30 dB. Threshold currents (~3 mA) of the shallow-etch samples were slightly lower than those (~4 mA) of the mid-etch samples, as shown in Fig. 5.

For the deep-etch samples (etched deeper than 22 pairs, 4.3 μm), only a few of them operate as lasers with very small output power. Since the top DBR had a total of 22 pairs of GaAs/$Al_{0.8}Ga_{0.2}$As layers, the air-holes were drilled deeper than the active region.

#3764 - $15.00 US Received 3 February 2004; revised 25 February 2004; accepted 26 February 2004

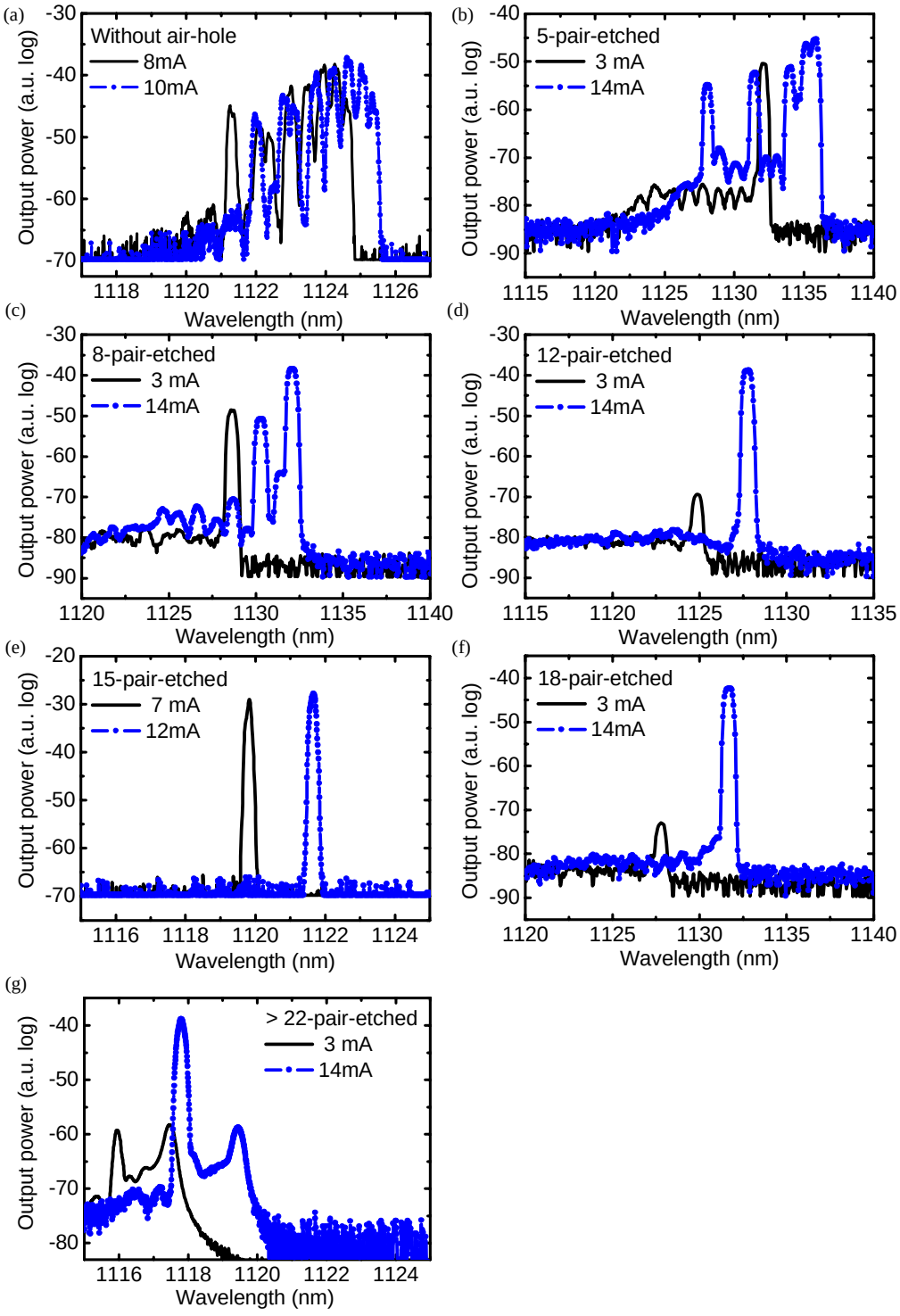

Fig. 2. Spectra of the rectangular air-hole PC-VCSELs with different air-hole depths of (a) 0, (b) 5, (c) 8, (d) 12, (e) 15, (f) 18, and (g) > 22 pairs, at just above- and above-threshold currents.

#3764 - $15.00 US Received 3 February 2004; revised 25 February 2004; accepted 26 February 2004

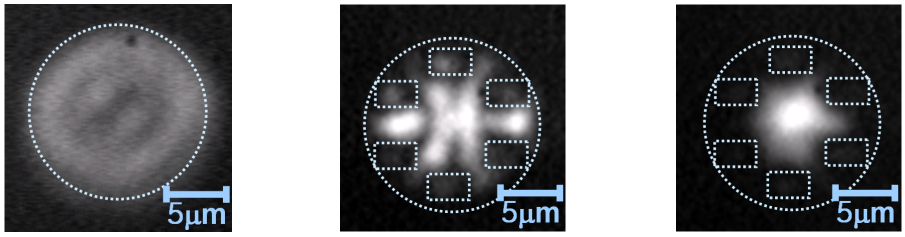

(a) (b) (c)

Fig. 3. Near-field CCD mode patterns. (a) Reference VCSEL. (b) Shallow-etch sample (8-pairs of $GaAs/Al_{0.8}Ga_{0.2}As$ etched layers, 12 mA). (c) Mid-etch sample (12 mA). In the CCD images, the circle indicates the inner boundary of the top electrode and the rectangles show positions of the air-holes.

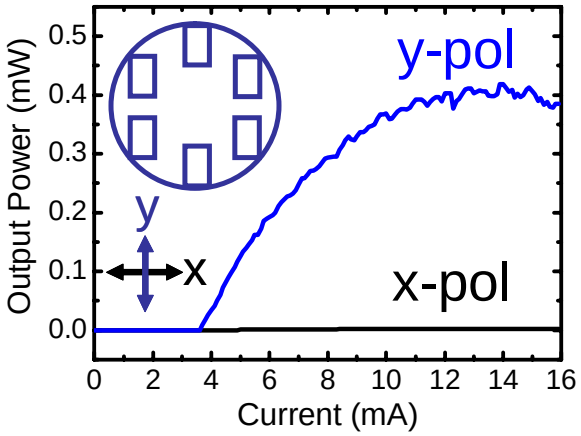

(a)

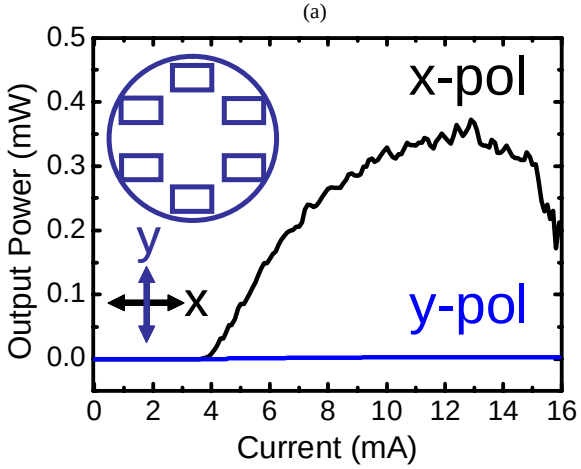

(b)

Fig. 4. Polarization resolved L-I curves of (a) vertically-oriented, and (b) horizontally-oriented air-hole PC-VCSELs.

#3764 - $15.00 US Received 3 February 2004; revised 25 February 2004; accepted 26 February 2004

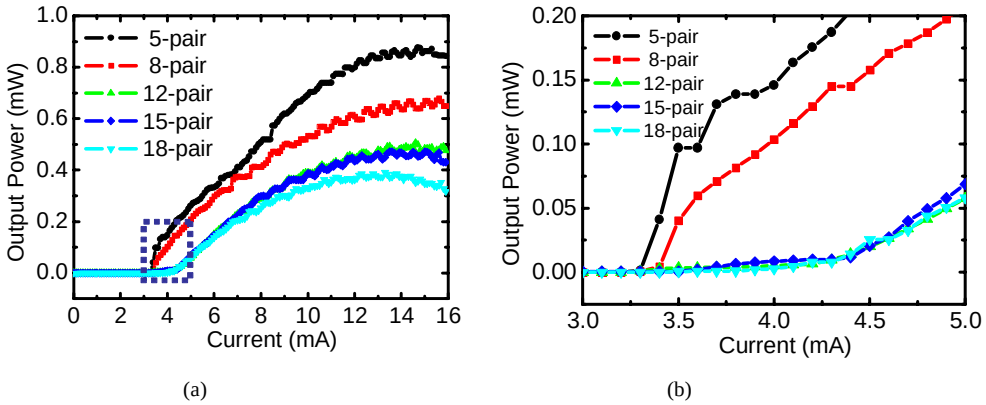

Fig. 5. (a) L-I curves of the PC-VCSELs with different air hole depths. (b) L-I curves of the near threshold currents.

Therefore, the surface recombination became non-negligible and was responsible for the poor performance as a laser. However, it is interesting to note that the threshold current (~2.5 mA) was even smaller than that of the shallow etch samples. Moreover, the deep-etch laser functions in the multi-modes in the entire operating range and it never finds itself in the fundamental single mode as shown in Fig. 2(g).

4. Analysis

The stable single transverse mode operation observed from various the mid-etch samples implies a very large fabrication tolerance of this PC-VCSELs. To understand this encouraging issue, one needs to study the general mode selection mechanisms for PC-VCSELs.

As a first step, we computed the photonic-crystal-guided (PC-guided) modes by the plane wave expansion method employing the simplified photonic crystal structure. An air-hole photonic crystal waveguide structure of high refractive index 3.25 was used as a model structure as shown in Fig. 6(a). Two perfect mirrors were placed at the top and bottom boundaries for simplicity. Through the analyses, we found the existence of a total of three PC-guided transverse modes in the model PC structure as shown in Figs. 6(b) – (d). This finding suggests the possibility of a maximum of three PC-guided transverse modes in the partly-drilled real PC-VCSEL structure. Note that this situation is different from the endless-single-mode holey fiber where only one transverse mode is allowed [13], possibly because of the high refractive index of the host material and large air-hole size. The size of the computational super-cell was $5\Lambda \times 3\sqrt{3}\,\Lambda$ where Λ is the air-hole pitch.

To experimentally verify the existence of the higher order PC-guided modes, we tried to measure the spectral separation of the two right-most peaks. In fact, in the typical above-threshold spectrum, the very faint 2nd-order PC-guided peak was hardly visible in the shadow of the strong single peak representing the lasing of the fundamental (1st-order) PC-guided mode. However, near the threshold where the mode competition was not as strong, those weak non-lasing nearby peaks became visible and the spectral separation could actually be measured. The measured spectral separation of the two right-most modes lies between 4.3 - 6.7 Å as shown in Fig. 7. Here, each dot denotes the mean value of the spectral mode separation measured from four PC-VCSELs of the same etch depth. It is encouraging to observe that the measured spectral separation (~ 6.7 Å) of the deep-etch sample approached that (10 Å) computed from the plane wave expansion method with the fully-drilled model structure. For the mid-etch samples, this photonic crystal index guiding effect corresponded to the effective index difference (Δn) of 0.003 ~ 0.004 between the core and cladding regions.

#3764 - $15.00 US Received 3 February 2004; revised 25 February 2004; accepted 26 February 2004

The peak corresponding to the third transverse PC-guided mode was invisible even near the threshold, which is attributed partly to the large mode size that overlaps much more with the absorptive region of the quantum wells.

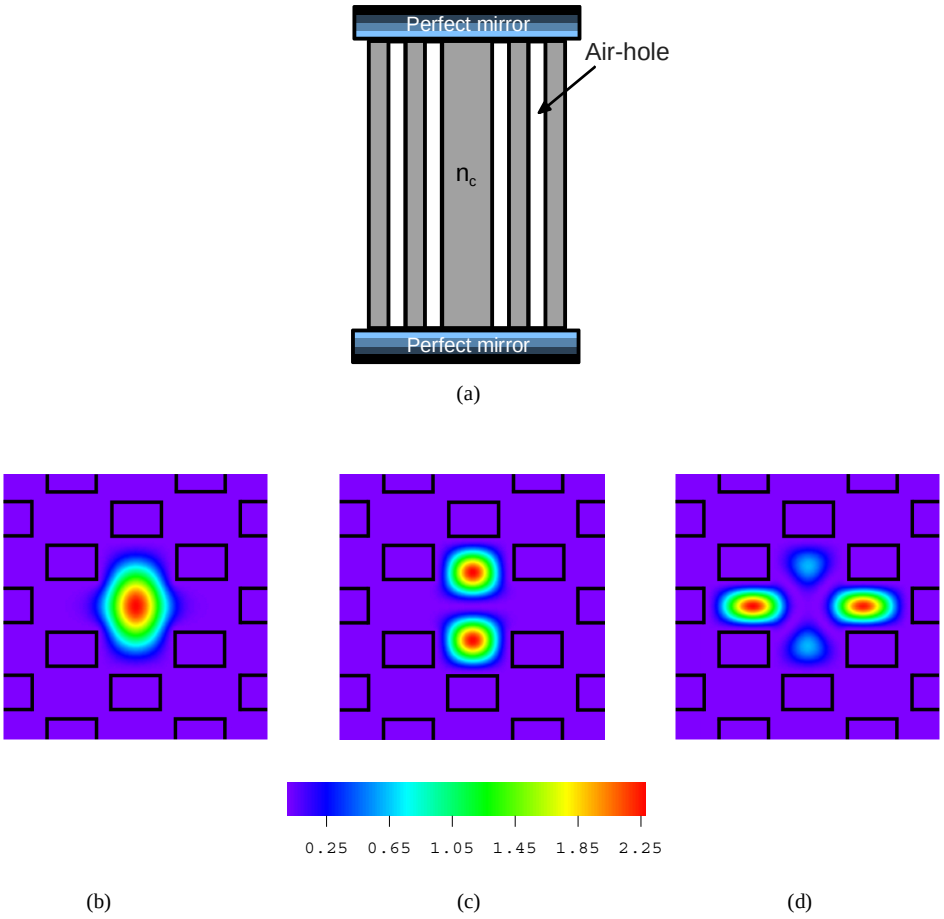

Fig. 6. (a) The waveguide structure used to calculate the mode profiles. n_c = 3.25. (b) Fundamental (1st-order) PC-guided mode. (c) 2nd-order PC-guided mode. (d) 3rd-order PC-guided mode.

Now we tried to explain the mode competition and selection mechanisms that are strongly correlated with the modal gain and loss. For the PC-VCSELs with identical current injection scheme with different etch depths, the material gain profiles could be assumed to be the same. Under this circumstance, the modal loss would become the dominant factor for the mode selection. To estimate the modal loss for the PC-guided modes, information on the size and the shape of the mode and the etch-depth dependent mirror loss is needed. The measured values of the mode size were slightly larger than those obtained from the computation by 2.2 ~ 6.0 % depending on the air-hole depths. As mentioned previously, the mode size of PC-VCSELs decreased with the etch depth. This monotonic decrease of the mode size could be explained as a consequence of the monotonic increase of the index guiding effect with the etch depth. This difference between the experiment and the computation could be attributed to the finite depth of the air-hole in the real PC-VCSELs as compared to the completely penetrated structure employed in the model. For simplicity, we assumed and used the computed mode profile, which is then scaled by the experimentally measured mode size for our future analyses.

#3764 - $15.00 US Received 3 February 2004; revised 25 February 2004; accepted 26 February 2004

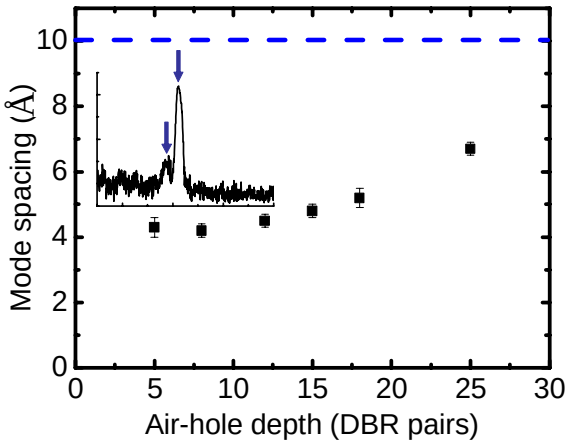

Fig. 7. Measured spectral separation between the fundamental and 2nd-order PC-guided modes. The right-most data point was positioned after converting the physical depth (4.3 μm) into the number of DBR pairs. The dashed line is the asymptotic value from the plane wave expansion method with the fully-drilled model structure. The inset figure is a spectrum of the mid-etch sample below-threshold current (2 mA), showing the two PC-guided modes.

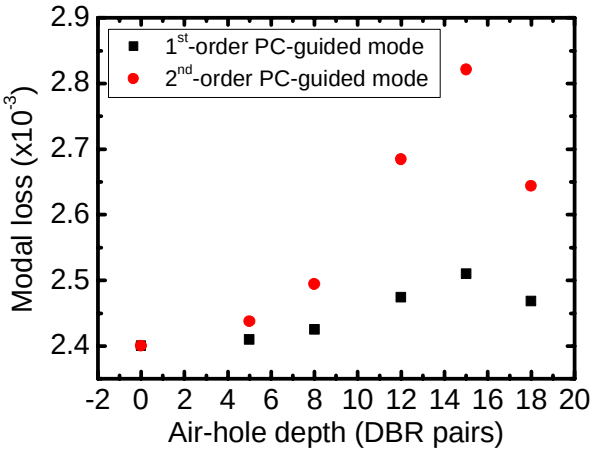

Fig. 8. Modal losses of the 1st-order and 2nd-order PC-guided mode versus air-holes depth.

For the PC-VCSEL with spatially non-uniform top mirror, the modal loss depends strongly on the size and the shape of the mode. For example, the large high-order modes would have more overlap with the air-hole region where the reflectivity is low and the optical loss is large. For the shallow-etch samples, the small fundamental mode won the competition in the beginning. However, with higher current injection providing slightly increased material gain, the higher-order modes could also reach the lasing condition when the reflectivity modulation was not strong enough. The situation became different for the mid-etch samples. In this case, because of the moderated etch depth, the reflectivity of the top DBR became strongly degraded. The small difference in the mode size and shape between the two lowest modes resulted in the non-negligible modal loss difference. As mentioned previously, the size of the fundamental mode decreased with the etch depth. This was also the case for the 2nd-order PC-guided modes. At the same time, the reflectivity of the top mirror decreased strongly with the etch depth of the top DBR. With this in mind, we computed the net modal loss difference as a

#3764 - $15.00 US Received 3 February 2004; revised 25 February 2004; accepted 26 February 2004

function of the air-hole depth using the measured mode size as summarized in Fig. 8. The modal loss was calculated using the Eq. (1).

$$Modal\ Loss = \frac{\int_{cross-section} \varepsilon(\mathbf{r})\left|\mathbf{E}(\mathbf{r})\right|^2 \left(1-R(\mathbf{r})\right) d\mathbf{r}}{\int_{cross-section} \varepsilon(\mathbf{r})\left|\mathbf{E}(\mathbf{r})\right|^2 d\mathbf{r}} \quad (1)$$

Where ε, $\mathbf{E}$, and R are the permittivity, the electrical field amplitude of each mode, and the position-dependent reflectivity of the etched DBR mirror, respectively.

For the mid-etch samples, the modal loss difference was large enough for the effective mode selection. These devices operated in a fundamental transverse mode over the entire operating current range as observed. Interestingly, the loss difference did not increase monotonically with the air-hole etch depth and showed maximum when the etch depth was 15 pairs. Therefore, the optimal air-hole depth for the single transverse mode operation was likely to be around 15 pairs. In general, the deep-etch samples were very unstable and it was not easy to obtain reliable data. However, the threshold current tended to be slightly smaller than the mid-etch samples, indicating reduced modal losses. In the near threshold current regime, both the PC-guided mode and the oxide-guided modes participated in the competition. As current increased, the modal characteristics became complicated and sometime those modes other than PC-guided mode were also observed.

5. Conclusion and summary

We have controlled the transverse mode by etching depth tuning in 1120-nm highly-strained GaInAs/GaAs rectangular air-hole PC-VCSELs. The single-polarization, single-transverse-mode operation over the entire operating current range was obtained over a wide range of the etch depth of 12- ~ 18-pairs. Through a comparison based on the measurement and the simulation, we argued the existence of a maximum of three possible PC-guided modes in the long wavelength end of the emission spectra. The shallow-etch samples did not maintain the single transverse mode because of the insufficient index-guiding effect and insufficient modal loss difference. In comparison, for the mid-etch samples, the size of the PC-guided mode decreased with the depth of the etched air-hole, stemming from the etch-depth-dependent index guiding effect. The sufficient modal loss difference between the two lowest PC-guided modes was large enough to support the single transverse mode operation over the entire operating current range. The wide range of the air-hole depth for the single transverse mode operation enables easy mode control, and makes PC-VCSELs easily manufacturable single mode light sources.

Acknowledgments

This work was supported by the National Research Laboratory project of KISTEP, Korea.

#3764 - $15.00 US Received 3 February 2004; revised 25 February 2004; accepted 26 February 2004